Phased Array Networking TT&C Relay Terminal with Interference Suppression Technology

Liu Liu[1,2], Tian Liu[2], Yang Li[3], Wensheng Pan[3], and Yan Zhang[1(✉)]

[1] School of Communication Engineering, Xidian University, Xian 710071, China
yanzhang@xidian.edu.cn
[2] Southwest China Institute of Electronic Technology, Chengdu 610036, China
[3] National Key Laboratory of Wireless Communications, University of Electronic Science and Technology of China, Chengdu 611731, China

Abstract. This article aims at the interference suppression problem of full-duplex relay terminals in the telemetry, tracking and command (TT&C) network system, analyzes the interference signal characteristics and the delay expansion of the self-interference signal when the transmitting and receiving antenna arrays are separated, and analyzes the interference in sub-arrays of different sizes. To solve the signal delay expansion, a kind of interference suppression method is proposed after the combination of array antenna reception beamforming. This method expands the delay range according to the layout of the array and the delay expansion of interference signals in sub-arrays of different sizes. All array elements are equivalent to one array element, which greatly reduces the complexity of radio frequency suppression. Theoretical analysis and simulation experimental results show that this method can effectively suppress interference signals. For the scenario of 256 array element transmitting front and 256 array element receiving front, the simulation compared the interference suppression performance under different tap numbers. The simulation results show that using 16 taps can suppress interference with a carrier frequency of 26.8 GHz and a bandwidth of 200 MHz. The signal suppression capability is greater than 47 dB.

Keywords: Phased array · network measurement and control · relay terminal · full-duplex · radio frequency interference suppression

1 Introduction

With the rapid development of unmanned platform technologies, the number of large-scale constellations, star clusters, and formations is constantly increasing, giving rise to an urgent need for a pervasive and all-time TT&C communication network. As the sole channel connecting ground stations with aircraft, the TT&C communication system plays a pivotal role in transmitting flight instructions, equipment status, and reconnaissance data. Its stability and reliability are crucial for maintaining the normal operation of the entire network.

X. Li et al. (Eds.): SmartGift 2024, LNICST 600, pp. 20–35, 2025.
https://doi.org/10.1007/978-3-031-78806-2_2

However, under the conditions of large-scale and wide-area distribution, the varying distances and visible fields of view between aircraft result in significant dynamic variations in wireless link attenuation, leading to high probabilities of measurement and control interruptions and limited durations [1, 2]. To address this issue, the introduction of relay nodes has proven to be an effective solution. By strategically positioning relay nodes, it is possible to forward telemetry and telecommand information, maintain the continuity of tracking and orbit measurement, and establish a distributed networking TT&C communication system based on relay nodes, realizing all-time and pervasive interconnectedness [3–7].

Existing unmanned platform networking TT&C systems typically employ frequency-division duplexing (FDD) or time-division duplexing (TDD) for duplexing. Nevertheless, these approaches are associated with complexities in frequency pairing and limitations in channel capacity. In contrast, co-frequency co-time full-duplex (CCFD) wireless communication technology enables concurrent transmission and reception on the same frequency, facilitating more flexible spectrum allocation and usage, as well as improved channel utilization efficiency and networking access timeliness. Therefore, the application of CCFD technology in large-scale distributed networking TT&C communication systems holds significant promise [9, 10].

The utilization of millimeter-wave signals, characterized by high frequencies, short wavelengths, and miniaturized antenna sizes, has enabled the deployment of millimeter-wave multi-antenna systems on aircraft. While system energy consumption may increase with the expansion of antenna arrays, the directional beamforming capabilities of multiple antennas not only enhance transmission distances but also provide anti-interference and low-intercept characteristics, thereby bolstering network reliability and security [11]. Consequently, millimeter-wave multi-antenna CCFD technology is poised to become a crucial technology for relay nodes in future distributed networking TT&C communication systems.

However, multi-antenna co-frequency transceiver systems face more complex self-interference issues. The self-interference generated by multiple transmit antennas couples and superimposes on the receive antennas [12, 13], potentially leading to saturation and blocking of the receiver's radio frequency (RF) front-end. Furthermore, the analog-to-digital converter (ADC) after receive beamforming is more sensitive compared to the low-noise amplifier (LNA), imposing stricter requirements on the dynamic range of the received signal. This elevates the demand for self-interference suppression in array antennas.

Existing self-interference suppression techniques primarily encompass spatial self-interference suppression [14–21], digital self-interference suppression [22–24], and RF self-interference suppression [25–27]. While these techniques have demonstrated a certain degree of effectiveness in mitigating self-interference, challenges remain. Particularly in phased array systems, the numerous transmit and receive antenna elements give rise to a more intricate self-interference scenario, complicating the task of RF interference suppression. Currently, there is a dearth of research on RF interference suppression techniques specifically tailored for phased arrays, which poses a bottleneck for the practical application of phased array full-duplex technology.

To address this gap, this paper proposes an RF self-interference suppression method tailored for phased array networking TT&C relay terminals. This method is primarily applied after receive beamforming and before the signal enters the receiver's mixing stage. By suppressing the combined self-interference, it aims to prevent saturation of the down-conversion channel and reduce the demand for dynamic range in the receiver channel. Given the vast number of transmit and receive antennas and the varying spatial positions of the array elements, the self-interference signal often contains multiple strong direct paths. To address this, the proposed method leverages the concept of merging self-interferences with different delays within the relevant bandwidth into a single interference. By appropriately grouping antennas with similar delay differences due to their spatial positions and selecting an appropriate number of taps for suppression, the method effectively mitigates self-interference.

2 System Model

2.1 Phased Array Network Measurement and Control Relay Terminal Usage Scenarios

The usage scenario of the phased array network measurement and control relay terminal is shown in Fig. 1. Network 1 and Network 2 are different communication networks at the same operating frequency. Network 1 needs to exchange information with Network 2, due to the long distance between the networks, but direct communication cannot be accomplished, so a relay terminal is required.

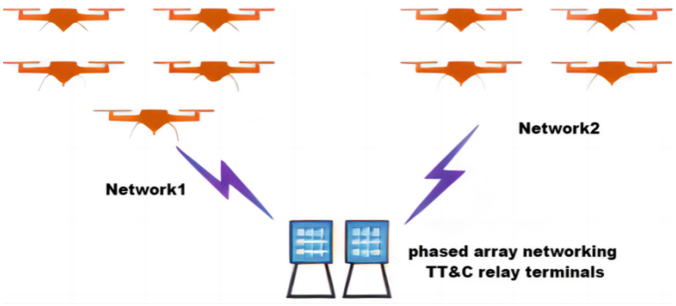

Fig. 1. Usage scenarios of phased array networking TT&C relay terminals

The phased array network measurement and control relay terminal uses the same frequency as Network 1 and Network 2 to receive the information from Network 1 and forward it to Network 2 to complete the relay function. At this time, the transmission and reception of the phased array network measurement and control relay terminal work at the same time, and the transmission and reception work at the same frequency. In order to ensure the normal operation of the relay terminal, the transmitter coupling signal needs to be suppressed at the receiving end.

2.2 Phased Array Network Measurement and Control Relay Terminal System Model

Figure 2 shows the structural block diagram of the phased array network measurement and control terminal. After the signal transmitted from the remote end is received by the receiving antenna, it is sent to the receiving link for processing and digital signal processing. The processed digital signal passes through the transmitting link and the transmitting antenna is sent out to complete the relay. In this system, the same frequency is used for reception and transmission. The receiving antenna not only receives the small signal from the remote end, but also receives the strong radio frequency signal transmitted and forwarded by the terminal itself. The transmitted signal causes strong interference to the received signal, so the receiver needs suppress the received self-interference signal, otherwise the remote signal cannot be correctly demodulated. In order to reduce the impact of co-channel interference on received signals, antenna isolation technology, digital interference cancellation technology and radio frequency interference cancellation technology are usually used. This article studies radio frequency interference suppression technology for phased array array antennas.

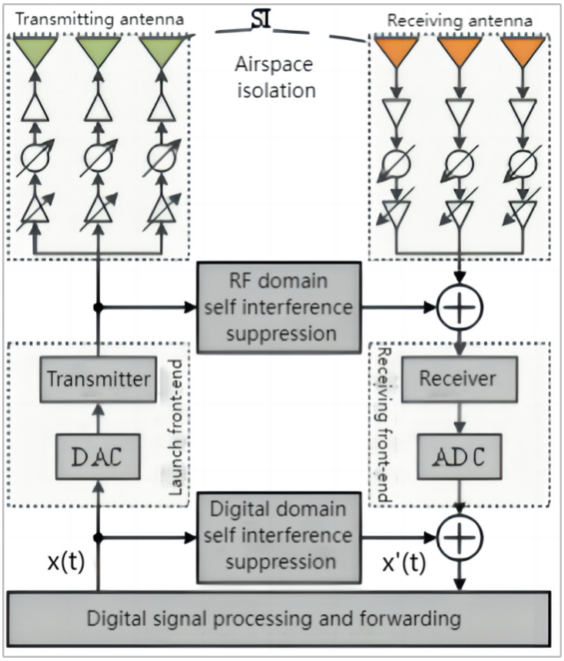

Fig. 2. Structure of phased array networking TT&C terminal architecture

2.3 Phased Array Self-interference Signal Model

For a transceiver antenna using a phased array of $P \times Q$ array elements placed in the same plane, the model is shown in Fig. 3. Suppose the (1,1) lattice element is the reference

array element, establish a Cartesian coordinate system based on the reference array element, d_x is the horizontal spacing, d_y is the vertical spacing, for any beam direction (φ, θ), φ is the direction angle, θ is the pitch angle.

The spatial phase difference of other array elements relative to the (1,1) lattice element is

$$\Delta\phi_{i,k} = \frac{2\pi}{\lambda}\big((i-1)d_x \cos\varphi \cos\theta + (k-1)d_y \sin\varphi \sin\theta\big) \tag{1}$$

Among them, λ is the signal wavelength, $i = 1...P$, $k = 1...Q$.

For the channel phase $\phi_{i,k}$ of any radiation array element, it can be expressed as:

$$\phi_{i,k} = \phi_{1,1} + \Delta\phi_{i,k} \tag{2}$$

For the (i,k)th array element of the transmitting antenna, its radiation signal complex radio frequency signal can be expressed as:

$$s_{i,k}(t) = \sqrt{p}x(t)e^{j2\pi f_c t} + d_{i,k}(t) + n_{i,k}(t) \tag{3}$$

Among them, $x(t)$ represents the equivalent baseband signal, $E\big(x^2\big) = 1$; f_c is the signal carrier frequency; $d_{i,k}(t)$ represents the nonlinear component of the signal transmitted by the (i, k)th array element; $n_{i,k}(t)$ represents the transmission noise of the (i, k)th array element; p is transmit power.

Due to the large path loss of millimeter waves and the short distance between the transmitting and receiving antennas, the self-interference signal caused by the multipath effect is relatively small. The self-interference signal studied in this article is caused by the direct path from the transmitting array element to the receiving array element.

For the receiving array, the self-interference signal received by the (i,k)th receiving array element can be expressed as:

$$r_s(t)_{m,n} = \sum_{i=0}^{P}\sum_{k=0}^{Q}\left(l_{i,k}^{m,n}s_{i,k}(t - \frac{d_{i,k}^{m,n}}{c})\right) \tag{4}$$

Among them, $l_{i,k}^{m,n}$ is the path loss factor from the (i,k)th transmitting array element to the (m,n)th receiving array element; $d_{i,k}^{m,n}$ is the transmission from the (i,k)th transmitting array element to the (m,n)th receiving array element. The distance, $d_{i,k}^{m,n}$ can be expressed as:

$$d_{i,k}^{m,n} = \sqrt{[D + (P - m + i - 1)d_x]^2 + \big[(k-n)d_y\big]^2} \tag{5}$$

Then the self-interference signal synthesized by receiving beamforming can be expressed as:

$$r_s(t) = \sum_{m=1}^{P}\sum_{n=1}^{Q}\sum_{i=1}^{P}\sum_{k=1}^{Q}\left(\omega_{m,n}l_{i,k}^{m,n}s_{i,k}(t - \frac{d_{i,k}^{m,n}}{c})\right) + n_r(t) \tag{6}$$

Among them, $\omega_{m,n}$ is the receiving beamforming factor of the (m,n)th receiving array element; $n_r(t)$ is the thermal noise of the receiving channel.

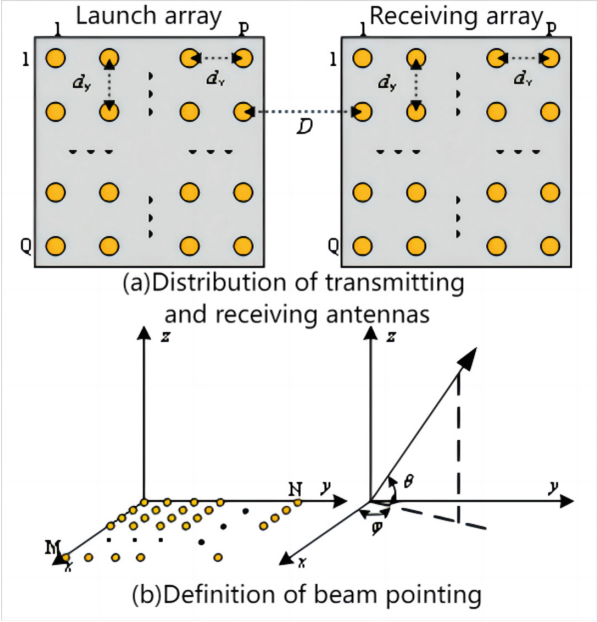

Fig. 3. Phased array transceiver array model

It can be seen from the formula that the self-interference signal synthesized after receiving is composed of P^2Q^2 signals with different amplitudes, delays and phases. The combined self-interference signal has rich multipaths and high power, which affects the dynamic range of the receiver and needs to be canceled in the radio frequency domain so that the receiving channel can normally receive small signals from the far end [13].

2.4 Multi-antenna Self-interference RF Suppression

The radio frequency interference suppression architecture is shown in Fig. 4 [30]. Before the transmit signal is sent to the terminal active phased antenna array, the coupling part of the transmit signal is used as a reference signal for radio frequency interference suppression. The reference signal is adjusted by multi-tap phase amplitude with different delays. Finally, they are combined together as a self-interference reconstructed signal.

The core content of radio frequency self-interference cancellation is radio frequency self-interference reconstruction. To improve the radio frequency self-interference cancellation capability, it is necessary to optimize the channel response of the reconstructed channel, so as to minimize the amplitude-frequency response of the equivalent channel response obtained by superimposing the received signal and the radio frequency self-interference reconstructed signal. The basic parameters of radio frequency self-interference reconstruction include the number of taps, delay, amplitude and phase. By adjusting the parameter values, the construction of different reconstructed channels can be achieved.

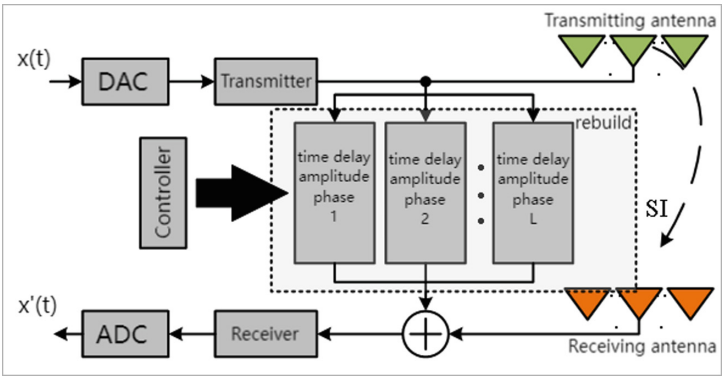

Fig. 4. RF self-interference suppression model

In the radio frequency self-interference suppression model, the reference signal is:

$$s_{ref}(t) = \sqrt{p_{ref}}x(t) + n_{ref}(t) \tag{7}$$

Among them, $n_{ref}(t)$ represents the thermal noise of the reference signal; p_{ref} is the power of the reference signal. Then the signal output by self-interference reconstruction is

$$s_{re}(t) = \sum_{l=1}^{L}\left(\alpha_l s_{ref}(t-\tau_l)e^{j\varphi_l} + n_{re,l}(t)\right) \tag{8}$$

Among them, L represents the number of taps of the reconstructed channel; α_l is the attenuation of the l th reconstructed tap; τ_l is the delay of the l th reconstructed tap; φ_l is the phase of the l th reconstructed tap; $n_{re,l}(t)$ is the noise of the l th reconstructed tap.

Then the signal after cancellation is

$$\begin{aligned} r_c(t) &= r_s(t) - s_{re}(t) \\ &= \sum_{m=1}^{P}\sum_{n=1}^{Q}\sum_{i=1}^{P}\sum_{k=1}^{Q}\left(\omega_{m,n}l_{i,k}^{m,n}s_{i,k}(t-\frac{d_{i,k}^{m,n}}{c})\right) + n_r(t) \\ &\quad - \sum_{l=1}^{L}\left(\alpha_l s_{ref}(t-\tau_l)e^{j\varphi_l} + n_{re,l}(t)\right) \end{aligned} \tag{9}$$

It can be seen from the equation that it is difficult to complete the reconstruction of the self-interference signal using one or a small number of reconstruction taps and obtain better cancellation performance. If one reconstruction tap is used to correspond to a self-interference signal of a specific amplitude and phase, P^2Q^2 reconstruction taps need to be used. Although better RF cancellation performance can be obtained at this time, the RF cancellation module will be bulky and the cost will increase. It has no practical significance in engineering.

Since the signal coupling between transceiver elements at different locations experiences different delays in space, for the synthesized self-interference signal, the superposition of several signal components with different delays will make the spectrum of the broadband self-interference signal appear frequency selective., this phenomenon is equivalent to the multipath effect. When the reciprocal of the maximum delay difference between the transmitting and receiving array elements is much larger than the signal bandwidth, signals with different delay components can be equivalent to one path.

According to the formula, combined with Fig. 3, in the planar array antenna model, the transmission delay between the array elements in the same row as the P th column of the transmitting array and the 1st column of the receiving array is the smallest, that is, when $m = P$, $i = 1$, $k = n$, the minimum signal transmission delay is

$$\tau_{min} = D \Big/ c \tag{10}$$

The transmission delay between diagonally diagonal elements of the transceiver array is the largest, that is, when $m = 1$, $i = P$, $k - n = Q - 1$, the maximum signal transmission delay is

$$\tau_{max} = \sqrt{[D + (2P - 2)d_x]^2 + \left[(Q - 1)d_y\right]^2} \Big/ c \tag{11}$$

The maximum delay difference is

$$\tau_{d-max} = \sqrt{[D + (2P - 2)d_x]^2 + \left[(Q - 1)d_y\right]^2} \Big/ c - D \Big/ c \tag{12}$$

When $1/\tau_{d-max}$ is much larger than the signal bandwidth, a path can be used to fit the self-interference signal. However, in large-scale phased array antenna systems, the RF cancellation performance of one tap is limited.

For a sub-array of size $P_t \times Q_t$ in the transmitting array and a sub-array of size $P_r \times Q_r$ in the receiving array element, the minimum delay, maximum delay and maximum delay difference of signal transmission between the sub-arrays are respectively:

$$\tau'_{min} = [(P - P_t - i_0 + m_0 - 1)d_x + D] \Big/ c \tag{13}$$

$$\tau'_{max} = \sqrt{\left[\tau'_{min} \times c + (P_t + P_r - 2)d_x\right]^2 + \left[(k_0 + Q_t - n_0 - 1)d_y\right]^2} \Big/ c \tag{14}$$

$$\tau'_{d-max} = \tau'_{max} - \tau'_{min} \tag{15}$$

Among them, (i_0, k_0) is the reference point of the transmitting sub-array, (m_0, n_0) is the reference point of the receiving sub-array, and $n_0 \leq k_0$; the reference array element position and the sub-array scale satisfy the following constraint relationship:

$$\begin{aligned} &i_0 + P_t + 1 \leq P, m_0 + P_r + 1 \leq P \\ &k_0 + Q_t + 1 \leq Q, n_0 + Q_r + 1 \leq Q \end{aligned} \tag{16}$$

According to this constraint relationship, it is easy to prove that $\tau_{min} \leq \tau'_{min}$, $\tau_{max} \geq \tau'_{max}$, then $\tau'_{d-max} \leq \tau_{d-max}$, that is, the delay expansion of any pair of sub-arrays is smaller than the delay expansion of the entire array.

It can be seen from the formula that when the array element spacing is determined, the maximum delay difference of the sub-array has nothing to do with the carrier frequency. Therefore, multiple array elements with a similar distance can be regarded as an antenna unit group. Since the array elements of each antenna unit group are relatively concentrated and the spatial distance difference between the transmitting and receiving array elements is small, the self-interference signal between the transmitting and receiving unit groups can be simplified as It consists of a signal with a delay component, as shown in Fig. 5. The transmitting antenna is converted into $P_{Bt}Q_{Bt}$ transmitting sub-arrays, and the receiving antenna is converted into $P_{Br}Q_{Br}$ receiving sub-arrays.

After regionalizing the antenna array, the formula can be rewritten as:

$$\begin{aligned} r_c(t) &= r_s(t) - s_{re}(t) \\ &= \sum_{g=1}^{P_{BR}} \sum_{h=1}^{Q_{BR}} \left(\sum_{r=1}^{P_{Bt}} \sum_{z=1}^{Q_{Bt}} l_{r,z}^{g,h} s_{r,z}(t - \tau_{r,z}^{g,h}) \right) \\ &\quad - \sum_{l=1}^{L'} \left(\alpha_l s_{ref}(t - \tau_l) e^{j\varphi_l} + n_{re,l}(t) \right) + n_r(t) \end{aligned} \tag{17}$$

Among them, L' represents the number of taps of the channel that needs to be reconstructed after the array is regionalized; $\tau_{r,z}^{g,h}$ is the time delay for the signal to be transmitted from the (r, z) th transmitting subarray to the (g, h) th receiving subarray; $l_{r,z}^{g,h}$ is the transmission time from the (r, z) th transmitting subarray to the (g, h) th receiving subarray. The complex gain factor of the array includes the channel response between array elements and the shaping factor of the receiving array element.

It can be seen from the formula that after the model is simplified, the self-interference signal can be canceled by $P_{Br}Q_{Br}P_{Bt}Q_{Bt}$ taps. The number of taps is far less than P^2Q^2, which is easy to implement in engineering.

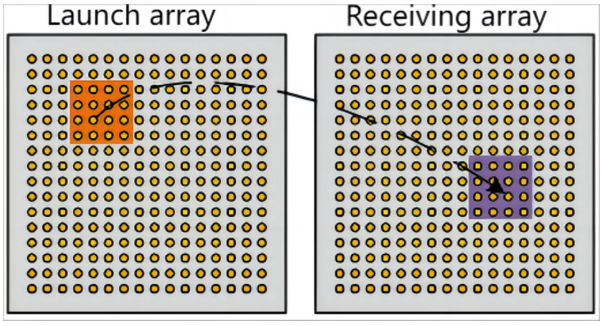

Fig. 5. Equivalent diagram of self-interference between subarrays

3 Verification and Application of RF Self-Interference Cancellation

To verify the research in the previous section, a simulation scenario is set and the performance of the phase control array self-interference and RF self-interference cancellation are simulated. The specific parameter settings of the simulation scenario are shown in Table 1.

Table 1. Simulation scenario parameters

Simulation parameters	Parameter description
Carrier center frequency	26.8 GHz
Signal bandwidth	200 MHz
Transmitter and receiver array scale	16 × 16
Element spacing	5.5 mm
Minimum spacing for transmitting and receiving elements	180 mm
Single element transmission power	6 dBm
Equivalent full-body radiation power of the transmitting array	54 dBm

3.1 The Power Distribution of the Self-interference in the Phase Control Array

Modeling the self-interference channel, and the signal power distribution of the receiver array is shown in Fig. 6 when the transmitting array sends.

Fig. 6. Power distribution of receiving array elements

Due to the symmetry relationship between the transmitting and receiving arrays, the received power of each receiver element also has a symmetry relationship. At this point, the received self-interference signals have relatively small power, and it will not cause the front-end low-noise amplifier to saturate.

When keeping the received array beam direction as the normal direction, scan the beam direction and azimuth for the transmitting array, and the power variation trend of

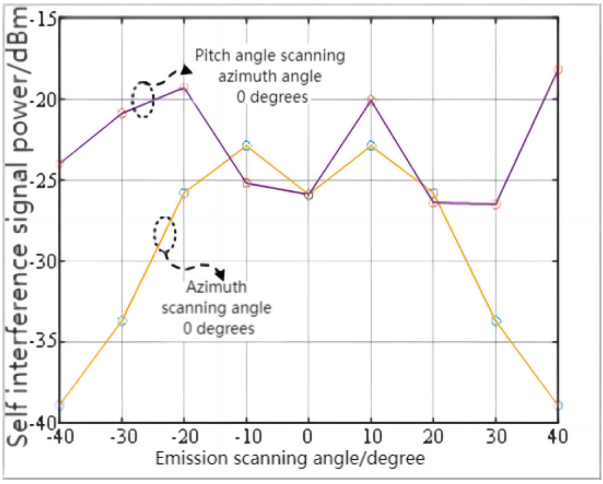

Fig. 7. Self-interference signal power in different directions

the largest self-interference signal in the receiver array is shown in Fig. 7. The maximum self-interference signal power in the receiver element is about −18 dBm.

3.2 Simulation of Frequency Self-interference Cancellation in Array Antennas

According to Eq. (17), divide the receiver and transmitter arrays into regions. Since the time expansion of different receive and transmit sub-arrays is inconsistent, the receive and transmit sub-array with the largest time expansion is selected as the reference sub-array. The maximum time expansion in different sub-array division as shown in Table 2 can be observed. It can be seen that as the number of sub-arrays in the receiver and transmit arrays increases, the time expansion between the receiver and transmit sub-arrays becomes smaller.

Table 2. Delay extension under different region partitioning

Launch array segmentation	Receive array segmentation	Delay extension
1 × 1	1 × 1	0.582 ns
1 × 1	2 × 2	0.441 ns
1 × 1	4 × 4	0.369 ns
2 × 1	2 × 1	0.441 ns
2 × 1	2 × 2	0.440 ns
2 × 2	2 × 2	0.299 ns
4 × 4	4 × 4	0.139 ns

Simulation Model

Figure 8 provides an ADS simulation block diagram for frequency independent interference cancellation based on the different sub-arrays of the transceiver array. The simulation network of the transceiver array simulates the self-interference channel of the transmission antenna to the received antenna with 256 × 256 channels of delay, phase, and attenuation. The signal reconstruction of the self-interference is simulated through the adjustment of the time delay, amplitude, and phase of each tap, aiming to achieve the minimum amplitude of the reconstructed self-interference signal. The number of tap, L, determines the number of channels in the transceiver array.

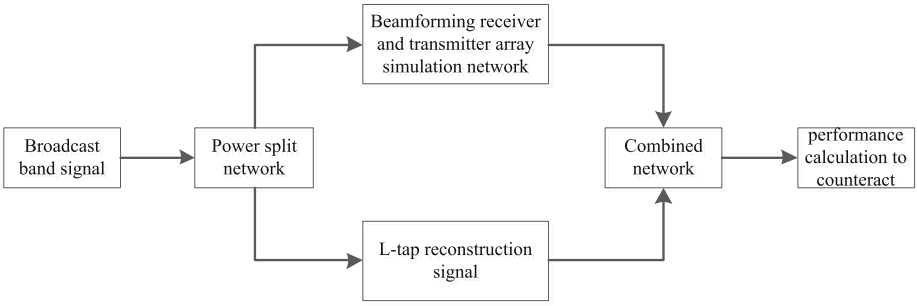

Fig. 8. ADS simulation block diagram

The signal source modulation method is 16QAM, and the simulation is conducted using the pulse-shaping method to optimize the frequency independent interference cancellation performance. According to the actual usage parameters of the device, the time interval of the tap is 10 ns, the phase shifter is 5.625°, and the attenuation factor is 0.5dB.

The transceiver array is simulated by replacing the transmit and receive arrays with 2 × 1, 2 × 1, and 2 × 2, respectively, and using 4, 8, and 16 taps to reconstruct the interference signal. The simulation of frequency independent interference cancellation performance is conducted.

The Simulation Results

In the direction of the line, the simulation results of the frequency independent interference cancellation performance of the transceiver array with different tap numbers are shown in Fig. 9, and the specific numerical results are presented in Table 3.

From the simulation results, it can be seen that as the number of tap in the transceiver array increases and the number of tap for the reconstruction of the tap increases, the performance of the self-interference cancellation gradually improves. When the 200 MHz bandwidth self-interference signal is reconstructed using 4 taps, the self-interference suppression ability is 21.5 dB; when the 200 MHz bandwidth self-interference signal is reconstructed using 16 taps, the self-interference suppression ability is 47.4 dB. The simulation results prove that the frequency independent self-interference cancellation

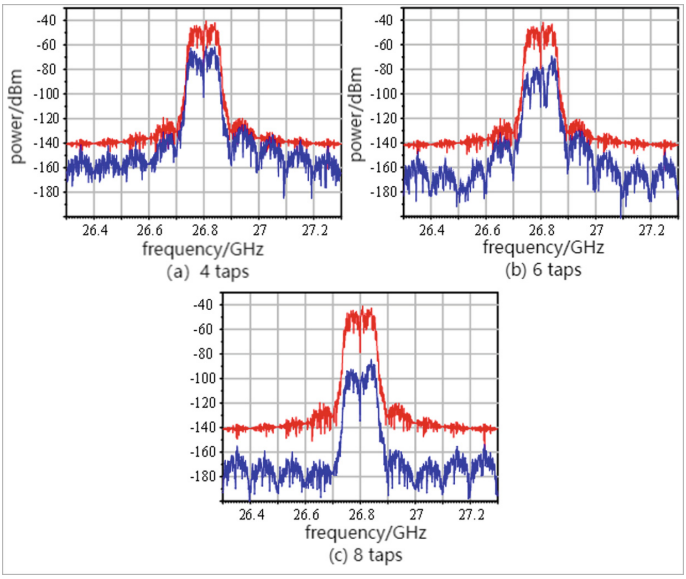

Fig. 9. Self-interference suppression performance with different taps

method with subarray division and a large reduction in the number of tap for the reconstruction of the tap can effectively suppress self-interference signals in the phase control array system.

Table 3. RF self-interference cancellation results with different tap numbers

Tap numbers	Offset before power	Offset after power	Quantum damping factor
4	−33.3 dBm	−54.8 dBm	21.5 dB
8	−33.3 dBm	−64.9 dBm	31.6 dB
16	−33.3 dBm	−81.0 dBm	47.7 dB

Similarly, keeping the beam direction of the receiver array fixed in the direction of the line, the beam scanning of the transceiver array is performed in the azimuth and elevation directions. The simulation results of the frequency independent interference cancellation performance of the transceiver array with different tap numbers are shown in Fig. 10. The results show that when the transceiver array scans in the same beam direction, the frequency independent interference cancellation ability of the transceiver array with the same number of taps in the reconstruction of the interference signal is similar.

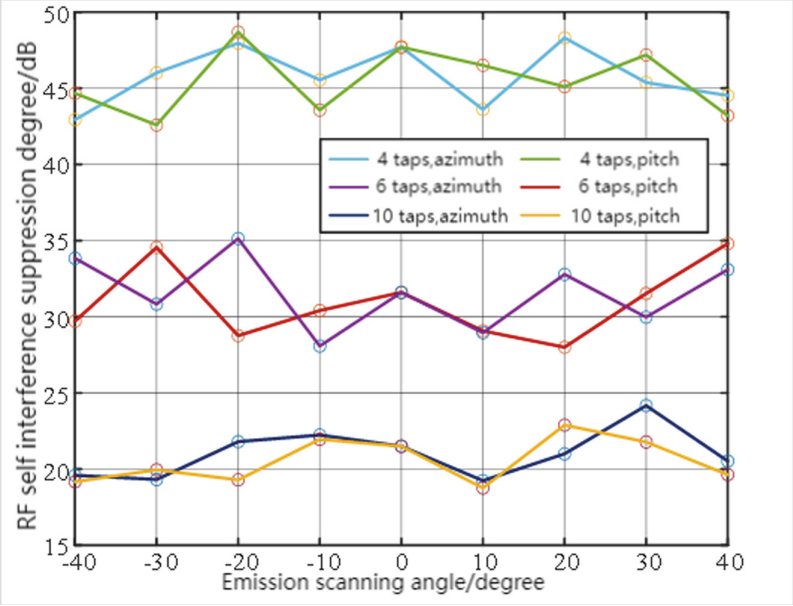

Fig. 10. Cancellation performance during transmitting beam scanning

Conclusion

In conclusion, this paper presents a comprehensive study on the self-interference issue in distributed network communication systems, specifically focusing on millimeter-wave large-scale array antenna scenarios. A simplified model for anti-self-interference suppression in arrays was proposed and validated through simulations, demonstrating its significant effectiveness in suppressing RF self-interference signals. Real-world testing further corroborated these results, achieving a suppression performance of over 47 dB under conditions of a 26.8 GHz central frequency and a 200 MHz self-interference bandwidth. This theoretical and experimental work establishes the foundation for frequency self-interference cancellation in large-scale array antenna network scenarios, paving the way for the application of concurrent frequency reception and transmission in future distributed networked testing and control systems.

References

1. Sivakumar, P., Singh, M., Malhotra J., et al.: Performance analysis of 160Gbit/s single-channel PDM-QPSK based inter-satellite optical wireless communication (IsOWC) system. Wireless Networks, **26**(5), 3579–3590 (2020). https://doi.org/10.1007/s11276-020-02287-2
2. Zhu, Z., Guo, Y., Zhong, C.: Distributed attitude coordination tracking control for spacecraft formation with time-varying delays. Trans. Inst. Measure. Control (2017). https://doi.org/10.1177/0142331217696146
3. El-Ferik, S., Hashim, H.A., Lewis, F.L.: Neuro-adaptive distributed control with prescribed performance for the synchronization of unknown nonlinear networked systems. IEEE Trans. Syst. Man Cybern. Syst. 1–10 (2017). https://doi.org/10.1109/TSMC.2017.2702705

4. Zhao, Z., Xu, G., Zhang, N., Zhang, Q.: Performance analysis of the hybrid satellite-terrestrial relay network with opportunistic scheduling over generalized fading channels. IEEE Trans. Veh. Technol. **71**(3), 2914–2924 (2022)
5. Ei, C.L., Jun, L., Wei, Z.: Distributed relay selection strategy for satellite-terrestrial cooperative system based on fairness. Comput. Eng. (2016)
6. Zeng, Y., Zhang, R.: Throughput maximization for UAV enabled mobile relaying systems. IEEE Trans. Commun. **64**(12), 4983–4996 (2016)
7. Srikanthakumar, S., Liu, C., Chen, W.H.: Optimization-based safety analysis of obstacle avoidance systems for unmanned aerial vehicles. In: International Conference on Unmanned Aircraft Systems (2012)
8. Samara, L., Ozdemir, O., Mokhtar, M., et al.: Analysis of in-band full-duplex OFDM signals affected by phase noise and I/Q imbalance. In: Qatar Foundation Annual Research Conference Proceedings (2016). https://doi.org/10.5339/qfarc.2016.ICTOP2684
9. Liu, Z.S., Zhou, Q.J., Gan, W.S., et al.: Adaptive joint channel estimation of digital self-interference cancelation in co-time co-frequency full-duplex underwater acoustic communication. In: 2019 IEEE International Conference on Signal, Information and Data Processing (ICSIDP). IEEE (2019). https://doi.org/10.1109/ICSIDP47821.2019.9173156
10. Bo-Lun, L.I., Tao, L., Ai-Wei, S.: Physical-layer security performance analysis of cooperative systems with energy harvesting-based relay. Commun. Technol. (2017)
11. Tahseen, H.U., Yang, L., Hongjin, W.: A dual-array antenna system for 5G millimeter-wave applications. Appl. Comput. Electromagn. Soc. J. **2021**(10), 36 (2021)
12. Jiang, H., Yu, Z., Yang, J.: Research on key technology of full duplex cognitive radio network. J. Phys. Conf. Ser. **1920**(1), 012035 (9pp) (2021). https://doi.org/10.1088/1742-6596/1920/1/012035
13. Mura, M.L., Bagolini, A., Lamberti, P., et al.: Extreme value analysis of the impact of the effective gap tolerance on the acoustic transmit and receive performance of reverse-CMUT arrays. In: 2022 IEEE International Ultrasonics Symposium (IUS), pp. 1–4 (2022). https://doi.org/10.1109/IUS54386.2022.9958299
14. Cacciola, R., Holzman, E., Carpenter, L., Gagnon, S.: Impact of transmit interference on receive sensitivity in a bi-static active array system. In: IEEE International Symposium on Phased Array Systems and Technology (PAST), pp. 1–5. Waltham, MA (2016)
15. Narbudowicz, A., Ruvio, G., Ammann, M.J.: Passive self-interference suppression for single-channel full-duplex operation. IEEE Wirel. Commun. **25**(5), 64–69 (2018). https://doi.org/10.1109/MWC.2018.1700236
16. Makar, G., Tran, N., Karacolak: A high isolation monopole array with ring hybrid feeding structure for in-band full-duplex systems. IEEE Antennas Wireless Propagat. Let. **16**, 356–359 (2016)
17. Shi, C., Pan, W., Shen, Y., Shao, S.: Robust transmit beamforming for self-interference cancellation in STAR phased array systems. IEEE Signal Process. Lett. **29**, 2622–2626 (2022)
18. Zhang, J., Zheng, J.: Prototype verification of self-interference suppression for constant-amplitude full-duplex phased array with finite phase shift. Electronics **11**(3), 295 (2022). https://doi.org/10.3390/electronics11030295
19. Liyanaarachchi, S.D., Barneto, C.B., Riihonen, T., et al.: Joint multi-user communication and mimo radar through full-duplex hybrid beamforming. In: 2021 1st IEEE International Online Symposium on Joint Communications & Sensing (JC&S).IEEE (2021). https://doi.org/10.1109/JCS52304.2021.9376319
20. Lopez-Valcarce, R., Gonzalez-Prelcic, N.: Analog beamforming for Full-duplex millimeter wave communication. In: International Symposium on Wireless Communication Systems. IEEE (2019). https://doi.org/10.1109/iswcs.2019.8877288
21. Kolodziej, K.E., Doane, J.P., Perry, B.T., Herd, J.S.: Adaptive beamforming for multi-function in-band full-duplex applications. IEEE Wirel. Commun. **28**(1), 28–35 (2021)

22. Kim, Y.J., Shin, J., Cho, H., et al.: Implementation of self-interference cancellation techniques for full-duplex communication. J. Korean Inst. Inform. Commun. Eng. **20**(3), 484–490 (2016). https://doi.org/10.6109/jkiice.2016.20.3.484
23. Zhang, Z., Shen, Y., Shao, S., et al.: Full duplex 2×2 MIMO radios. In: 2014 Sixth International Conference on Wireless Communications and Signal Processing (WCSP), pp. 1–6. IEEE (2014)
24. Ma, T., Lei, H., Xiang, X.: Digital self-interference cancellation in single channel full-duplex system. Semicond. Optoelectron. (2016). https://doi.org/10.16818/j.issn1001-5868.2016.03.024
25. Tytgat, L., Yaron, O., Pollin, S., et al.: Analysis and experimental verification of frequency-based interference avoidance mechanisms in IEEE 802.15.4. IEEE/ACM Trans. Network. **23**(2), 369–382 (2015). https://doi.org/10.1109/TNET.2014.2300114
26. Pawinee, M., Peerapong, U., Monthippa, U.: Self-interference cancellation-based mutual-coupling model for full-duplex single-channel MIMO systems. Int. J. Anten. Propagat. **2014**, 1 (2014). https://doi.org/10.1155/2014/405487
27. Tamminen J, et al.: Digitally-controlled RF self-interference canceller for full-duplex radios. In: 24th European Signal Processing Conference (EUSIPCO), pp. 783–787. Budapest, HUNGARY (2016)